

New Mercury Vanadium Phosphate Hydrate $\text{Hg}_{4-x}\text{O}_{1-y}(\text{VO})(\text{PO}_4)_2 \cdot \text{H}_2\text{O}$ with Unprecedented Tetrahedral Oxo-Cluster $[\text{Hg}_{\sim 4}\text{O}_{\sim 5}]$

E. Le Fur, R. Gautier, E. Furet, and J. Y. Pivan*

Département de Physicochimie, UPRES 1795, Ecole Nationale Supérieure de Chimie de Rennes, Institut de Chimie de Rennes, Campus de Beaulieu, Avenue du Général Leclerc, 35700 Rennes, France

Received March 25, 2002

The new mercury vanadium phosphate hydrate $\text{Hg}_{4-x}\text{O}_{1-y}(\text{VO})(\text{PO}_4)_2 \cdot \text{H}_2\text{O}$ has been synthesized under hydrothermal conditions. X-ray investigations led to orthorhombic symmetry, space group $P2_12_12_1$ (No. 19), $a = 6.3632(2)$ Å, $b = 12.4155(5)$ Å, $c = 14.2292(6)$ Å, $Z = 4$. The crystal structure was solved and refined from single-crystal diffractometer data to residuals $R[F^2 > 2\sigma F^2] = 0.039$, $R_w(F^2) = 0.055$. The VPO framework consists of infinite one-dimensional $[\text{VO}(\text{PO}_4)_2]_{\infty}$ chains with corner-connected VO_6 octahedra and PO_4 tetrahedra. The chains run along the [100] direction and are held together by the unprecedented tetrahedral cationic units $[\text{Hg}_{4-x}\text{O}_{1-y}]^{4+}$. Presence of Hg–Hg bonding contacts is proved from theoretical calculations.

Introduction

Over the last 10 years, intensive studies have been devoted to the V–P–O system under hydrothermal conditions that have resulted in a wide family of vanadium phosphates hydrates (MVPOs) with open structures. The growing number of publications on MVPOs reflects the physico-chemical potentialities of these solids in various areas such as catalysis, low dimensional magnetism, topotactic reactions through ionic exchange, and(or) intercalation chemistry of neutral species, and so forth. In addition, the MVPOs show a very important structural variability in relation to various connectivities between the vanadium and phosphorus polyhedra. Indeed, the variable coordination polyhedra around the vanadium ions (regular or distorted octahedra for V^{3+} , V^{4+} , and V^{5+} ; square planar pyramids for V^{4+} and V^{5+} , and so forth) and the different forms of the phosphate ions PO_4^{3-} , HPO_4^{2-} , and(or) H_2PO_4^- coupled to homo- and(or) hetero-condensation mechanisms during the synthetic processes open up numerous perspectives to the chemist for the working out of new porous frameworks. Mercury is known to adopt oxidation states that range from Hg^0 to Hg^{2+} , passing through monovalent dumbbells Hg_2^{2+} and polyatomic clusters Hg_n^{x+} .¹ The various dimensionality and topology of the latter species (isolated Hg_3^{4+} , linear or planar clusters Hg_n^{x+} ,

and so forth) make the mercury a promising template for the working out of new open framework solids. To the best of our knowledge, only two HgVPO phases have been isolated, namely $\text{HgV}_2(\text{P}_2\text{O}_7)$ (high-temperature solid-state reactions)² and $\text{Hg}_4\text{VO}(\text{PO}_4)_2$ (hydrothermal synthesis).³ Our investigations on the Hg–V–P–O system under hydrothermal conditions resulted in the synthesis of the title compound. We report herein the single-crystal study of the new mercury vanadium phosphate hydrate $\text{Hg}_{4-x}\text{O}_{1-y}(\text{VO})(\text{PO}_4)_2 \cdot \text{H}_2\text{O}$. Theoretical calculations are presented on the model compound $\text{Hg}_4\text{O}(\text{VO})(\text{PO}_4)_2$.

Experimental Section

Synthesis. Single crystals of the title compound were isolated as greenish needles from hydrothermal treatments of the reagents HgSO_4 (~1 mmol, 321.6 mg), V_2O_5 (~0.8 mmol, 153.5 mg), V (~1 mmol, 57.3 mg), 200 μL of ethylenediamine (~3 mmol), 1 mL of 85% H_3PO_4 (~15 mmol), and 3.5 mL of distilled water. All the reactants were manipulated in an extracting hood to prevent the toxicity of mercury species. The initial mixture was placed in a 23 mL Parr bomb, then heated at 463 K for 60 h under autogenous pressure, and slowly cooled to room temperature over a 2 day period. The final product was filtered off and recovered as a green powder that turned out to be in the majority $\text{Hg}_4\text{VO}(\text{PO}_4)_2$ from X-ray powder diffraction analysis.³ Single crystals were isolated under the microscope with different size, morphology (rods and

* To whom correspondence should be addressed. E-mail: jean-yves.pivan@ensc-rennes.fr.

(1) Pervukhina, N. V.; Magarill, S. A.; Barasov, V. V.; Romanenko, G. V.; Pal'chik, N. A. *Russ. Chem. Rev.* **1999**, *68* (8), 615.

(2) Boudin, S.; Grandin, A.; Leclaire, A.; Borel, M. M.; Raveau, B. *J. Mater. Chem.* **1994**, *4*, 1889.

(3) Le Fur, E.; Pivan, J. Y. *J. Solid State Chem.* **2001**, *158*, 94.

needles), and color. Further X-ray diffraction studies (Weissenberg analysis) revealed that these crystals corresponded to different phases, namely, the mercury vanadium phosphate $\text{Hg}_4\text{VO}(\text{PO}_4)_2$ with dumbbells Hg_2^{2+} (yellow-greenish crystals, rods) and the new compound $\text{Hg}_{4-x}\text{O}_{1-y}(\text{VO})(\text{PO}_4)_2 \cdot \text{H}_2\text{O}$ (greenish crystals, needles). Very few needles were present, and attempts to make $\text{Hg}_{4-x}\text{O}_{1-y}(\text{VO})(\text{PO}_4)_2 \cdot \text{H}_2\text{O}$ in quantitative yield were unsuccessful. In some experiments, small amounts of elemental mercury were also present.

X-ray Intensity Data Collection and Structure Determination.

Crystals suitable for structure determination were selected by visual examination under a microscope and mounted on thin glass fibers. Their quality was checked by preliminary Weissenberg studies. Single-crystal data collection was performed at room temperature using a Nonius Kappa CCD diffractometer with Mo $K\alpha$ radiation ($\lambda = 0.71073 \text{ \AA}$). The goniometer and detector angular settings were optimized using the Collect program.⁴ The data collection was performed in the $\kappa = 0$ and $\omega = 160^\circ$ configuration with the ω - ϕ mode using $\Delta\omega = \Delta\phi = 0.8^\circ$ rotation scans. The total exposure time was 338 min, and 323 frames were collected. The entire data set of 23705 reflections collected within the range $1^\circ < \theta < 35^\circ$ was indexed, corrected for Lorentz and polarization effects, and then integrated using the program Denzo from the Kappa CCD software package.⁵ Frame scaling, merging, and unit cell and orientation matrix determinations were performed using the program Scalepack.⁵ The crystal structure was solved with Sir97⁶ and refined against F^2 with the help of SHELXL-97.⁷ The entire structure model was easily obtained from subsequent difference Fourier maps. In the final steps of refinement, corrections for extinction effects were applied, and the anisotropic displacement parameters were refined together with the occupancy factors for all atoms. All the positions were found to be fully occupied ($0.96(2) < \tau < 1.00(2)$) with the exception of Hg4 ($\tau = 0.86(1)$) and O10 ($\tau = 0.74(2)$). So, solely the occupancy factors for Hg4 and O10 were allowed to vary in the last cycles leading to the final residuals of $R = 0.039$ and $R_w = 0.059$ ($w = 1/\sigma^2$), and the correct absolute structure was proved through the refined value of the Flack parameter 0.00(1). The most important electronic residues were located in the near vicinity of Hg2 at 0.84 and 0.29 \AA . The structural results reported herein have been obtained after the data were corrected for absorption ($T_{\min} = 0.219$, $T_{\max} = 0.362$) using the program Sortav.⁵ Further details of the data collection and refinement are listed in Table 1. Final atomic and thermal coordinates and selected bond distances and angles are listed in Tables 2 and 3. The structure drawings were produced using Diamond 2.0.⁸

Periodic Density Functional Calculations. The self-consistent ab initio band structure calculations of $\text{Hg}_{4-x}\text{O}_{1-y}(\text{VO})(\text{PO}_4)_2 \cdot \text{H}_2\text{O}$ were performed with the scalar relativistic tight binding linear muffin-tin orbital method in the atomic spheres approximation including the combined correction (LMTO).⁹ Exchange and correlation were treated in the local density approximation using the von Barth–Hedin local exchange correlation potential.¹⁰ Within the LMTO formalism, interatomic spaces are filled with interstitial spheres. The optimal positions and radii of these additional “empty

Table 1. Crystal Data for $\text{Hg}_{4-x}\text{O}_{1-y}(\text{VO})(\text{PO}_4)_2 \cdot \text{H}_2\text{O}$

Crystal Data	
empirical formula	$\text{Hg}_{4-x}\text{O}_{1-y}(\text{VO})(\text{PO}_4)_2 \cdot \text{H}_2\text{O}$
color; habit	greenish; needlelike
cryst syst	orthorhombic
space group	$P2_12_12_1$ (No. 19)
unit cell dimensions	$a = 6.3632(2) \text{ \AA}$ $b = 12.4155(5) \text{ \AA}$ $c = 14.2292(6) \text{ \AA}$
V	$1124.14(7) \text{ \AA}^3$
Z	4
fw	$1063.26 \text{ g} \cdot \text{mol}^{-1}$
density (calcd)	$6.282 \text{ g} \cdot \text{cm}^{-3}$
Data Collection	
crystal size (mm^3)	$0.25 \times 0.02 \times 0.02$
abs coeff	538.03 cm^{-1}
max 2θ	$2\theta \leq 70^\circ$
data collected	h : $-10, +10$ k : $-15, +20$ l : $-22, +22$
Structure Solution and Refinement	
unique data	4936
obsd data ($F^2 > 2.0\sigma(F^2)$)	4013
free params	167
R_{int}	0.072
residuals $R1^a$ ($F^2 > 2.0\sigma(F^2)$)	0.039
wR2	0.059
extinction coeff	0.00039(4)
min, max ($e/\text{\AA}^3$)	$-2.94, +4.17$
GOFF	1.298

$$^a R1 = \frac{\sum |F_o| - |F_c|}{\sum |F_o|}; wR2 = \frac{[\sum w(|F_o|^2 - |F_c|^2)/\sum w|F_o|^2]^{1/2}}{w} = 1/\sigma^2(F_o^2).$$

Table 2. Atomic Coordinates, Site Occupancy Factors (SOFs), and Equivalent Isotropic Displacement Coefficients $U(\text{eq})$ (10^2 \AA^2) with Their Standard Deviations in Brackets for $\text{Hg}_{4-x}\text{O}_{1-y}\text{VO}(\text{PO}_4)_2 \cdot \text{H}_2\text{O}$

atom	x	y	z	position	SOF	$U(\text{eq})$
Hg1	0.04828(5)	0.06330(3)	0.12674(2)	4a	1.0	1.82(1)
Hg2	0.56270(5)	0.99418(3)	0.04511(2)	4a	1.0	2.41(1)
Hg3	0.64806(5)	0.01765(3)	0.26529(3)	4a	1.0	2.37(1)
Hg4	0.86004(6)	0.80181(4)	0.14513(3)	4a	0.869(2)	2.29(1)
V1	0.2048(1)	0.8205(1)	0.3670(1)	4a	1.0	1.40(3)
P1	0.2429(3)	0.0475(2)	0.3717(2)	4a	1.0	1.90(5)
P2	0.7031(3)	0.7807(2)	0.4165(2)	4a	1.0	1.26(4)
O1	0.207(1)	0.9845(5)	0.4642(4)	4a	1.0	2.1(1)
O2	0.213(1)	0.9641(5)	0.2936(4)	4a	1.0	2.0(1)
O3	0.467(1)	0.0931(6)	0.3692(5)	4a	1.0	3.0(1)
O4	0.924(1)	0.6348(6)	0.1370(5)	4a	1.0	3.6(1)
O5	0.4897(7)	0.3432(5)	0.1190(4)	4a	1.0	1.9(1)
O6	0.1023(7)	0.3439(6)	0.1162(4)	4a	1.0	2.2(1)
O7	0.2980(8)	0.2742(5)	0.9765(4)	4a	1.0	1.9(1)
O8	0.209(1)	0.7379(5)	0.2795(4)	4a	1.0	2.5(1)
O9	0.3029(7)	0.1675(5)	0.1275(5)	4a	1.0	2.2(1)
O10	0.792(1)	0.9631(7)	0.1428(6)	4a	0.75(2)	2.9(3)
Ow	0.331(1)	0.7947(8)	0.0899(7)	4a	1.0	7.1(3)

spheres” (ES) were determined by the procedure described in ref 11. Twenty-seven nonsymmetry-related ESs with $0.75 \leq r_{(\text{ES})} \leq 2.22 \text{ \AA}$ were introduced in the calculations.

The full LMTO basis set consisted of 6s, 6p, 5d, and 4f functions for Hg, 4s, 4p, and 3d functions for V, 3s, 3p, and 3d functions for

(4) COLLECT: Kappa CCD software; Nonius BV: Delft, The Netherlands, 1998.

(5) Otwinowski, Z.; Minor, W. In *Methods in Enzymology*; Carter, C. W., Jr., Sweet, R. M., Eds.; New York: Academic Press: 1997.

(6) Altomare, A.; Burla, M. C.; Camalli, M.; Cascarano, G.; Giacovazzo, C.; Guagliardi, A.; Moliterni, A. G. G.; Polidori, G.; Spagna, R. *J. Appl. Crystallogr.* **1999**, *32*, 115.

(7) Sheldrick, G. M. *SHELXL-97, Program for crystal structure refinement*; University of Göttingen: Göttingen, Germany, 1997.

(8) Brandenburg, K. *J. Appl. Crystallogr.* **1999**, *32*, 1028.

(9) (a) Andersen, O. K. *Phys. Rev. B* **1975**, *12*, 3060. (b) Andersen, O. K. *Europhys. News* **1981**, *12*, 4. (c) Andersen, O. K. In *The Electronic Structure Of Complex Systems*; Phariseau, P., Temmerman, W. M., Eds.; Plenum Publishing Corporation: New York, 1984. (d) Andersen, O. K.; Jepsen, O. *Phys. Rev. Lett.* **1984**, *53*, 2571. (e) Andersen, O. K.; Jepsen, O.; Sob, M. In *Electronic Band Structure and Its Application*; Yussouf, M., Ed.; Springer-Verlag: Berlin, 1986. (f) Skriver, H. L. *The LMTO Method*; Springer-Verlag: Berlin, 1984.

(10) von Barth, U.; Hedin, L. *J. Phys. C: Solid State Phys.* **1972**, *5*, 1629.

(11) Jepsen, O.; Andersen, O. K. *Z. Phys. B: Condens. Matter* **1995**, *97*, 35.

Table 3. Selected Bond Lengths (Å) with Their Standard Deviations in Brackets and Bond Valence Sum (Σs) for $\text{Hg}_{4-x}\text{O}_{1-y}(\text{VO})(\text{PO}_4)_2 \cdot \text{H}_2\text{O}$

V1	O8	1.614(6)	Hg2	O10	2.053(8)
	O7	1.952(6)		O1	2.083(5)
	O5	1.974(5)		Ow	2.953(9)
	O6	1.990(5)		O9	2.955(6)
	O2	2.066(7)		O6	3.061(7)
	O1	2.461(7)		O4	3.172(7)
		$\Sigma(V1) = 4.01$			$\Sigma(\text{Hg2}) = 1.78$
P1	O4	1.522(7)	Hg3	O10	2.084(9)
	O3	1.532(6)		O3	2.097(6)
	O2	1.531(6)		O5	2.859(6)
	O1	1.548(6)		O2	2.877(5)
		$\Sigma(P1) = 5.02$		O8	2.970(7)
					$\Sigma(\text{Hg3}) = 1.70$
P2	O7	1.525(6)	Hg4	O10	2.048(9)
	O5	1.537(6)		O4	2.115(8)
	O6	1.538(6)		O8	2.993(6)
	O9	1.539(6)		Ow	3.098(8)
		$\Sigma(P2) = 5.00$			$\Sigma(\text{Hg4}) = 1.60$
Hg1	O10	2.062(8)	Hg3	Hg2	3.193(3)
	O9	2.075(5)			Hg3
	O1	2.851(6)	Hg4	Hg2	3.363(9)
	O2	2.873(6)	Hg2	Hg1	3.410(7)
	O7	2.961(6)	Hg3	Hg4	3.453(9)
	O8	2.996(6)	Hg1	Hg4	3.470(6)
		$\Sigma(\text{Hg1}) = 1.85$			

P, 2s, 2p, and 3d functions for O, and s, p, and d functions for ES. The eigenvalue problem was solved using the following minimal basis set obtained from Löwdin downfolding technique: Hg (6s, 6p, 5d, 4f), V (4s, 4p, 3d), P (3s, 3p), O (2s, 2p), and ES (1s). The k space integration was performed using the tetrahedron method.¹² Charge self-consistency and the average properties were obtained from 12 irreducible k points.

Structure Results and Discussion

The crystal structure of $\text{Hg}_{4-x}\text{O}_{1-y}(\text{VO})(\text{PO}_4)_2 \cdot \text{H}_2\text{O}$ (Figure 1) consists of interconnected VO_{5+1} distorted octahedra and P tetrahedra as frequently found in vanadium phosphate crystal chemistry. The asymmetric unit is given in Figure 2. Only heterocondensation occurs in $\text{Hg}_{4-x}\text{O}_{1-y}(\text{VO})(\text{PO}_4)_2 \cdot \text{H}_2\text{O}$, and the connectivity leads to chains with composition $[\text{VO}(\text{PO}_4)_2]_\infty$ that run along the a -axis. The vanadium atoms are coordinated to six oxygen atoms to form the well-known distorted octahedra VO_{5+1} characteristic of the vanadyl ion with a very short bond distance $\text{V}=\text{O}$ (O8) of 1.614(6) Å directed along [011], four basal distances of ca. 2.0 Å, and one long bond distance $\text{V}\cdots\text{O}$ (O1) of 2.461 (7) Å. The $\text{V}=\text{O}$ bonds from adjacent octahedra are trans to each other, and oxygen O8 is not shared with other polyhedra. The basal planes, grossly parallel to (011), are shifted from each other by about 1 Å, and each of the four oxygens is shared with PO_4^{3-} tetrahedra. It is worthwhile to note that oxygen O1 that makes the longer bond $\text{V}\cdots\text{O}$ at 2.461 (7) Å is strongly linked to Hg2 and P1. The vanadium polyhedron, connected to phosphate groups by sharing apexes (P2) and one edge (P1), is distorted with O—O edges ranging from ~ 2.8 (apex sharing) to ~ 2.5 Å (edge sharing). As a result, two sets of V—O—P bond angles at the shared O atoms occur depending on the way the different polyhedra are connected. The first set of values for apex sharing (138.18°, 138.69°, 146.06°)

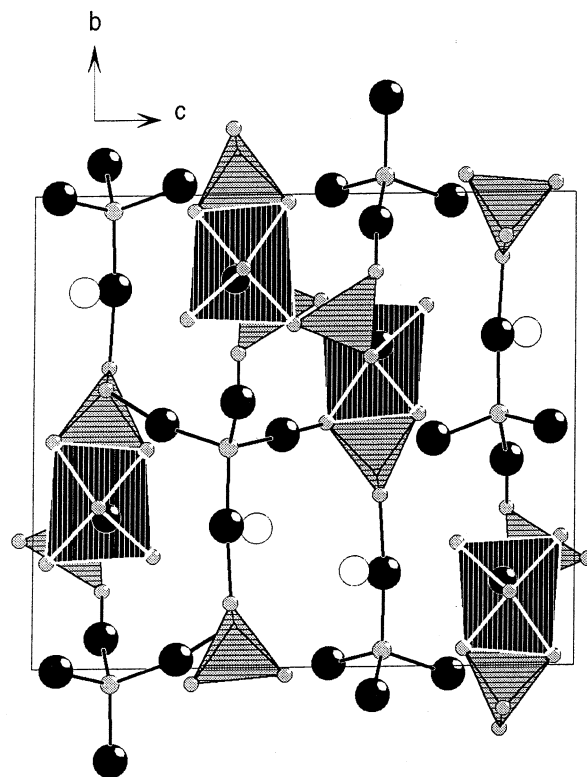


Figure 1. View of $\text{Hg}_{4-x}\text{O}_{1-y}(\text{VO})(\text{PO}_4)_2 \cdot \text{H}_2\text{O}$ along the [100] direction. The polyhedra are emphasized: black are VO_{5+1} octahedra; hatched are PO_4 tetrahedra. Black circles are the mercury atoms; gray and open ones are the oxygen atoms and water molecules.

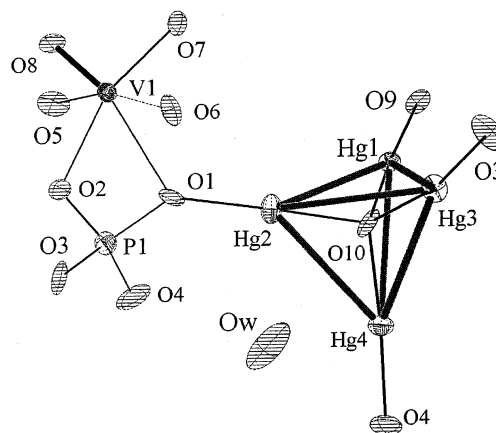


Figure 2. View of the asymmetric unit of $\text{Hg}_{4-x}\text{O}_{1-y}(\text{VO})(\text{PO}_4)_2 \cdot \text{H}_2\text{O}$ (ORTEP-style) showing the connectivity. Thermal ellipsoids are at the 50% probability level.

agrees fairly well with known values for μ_2 -oxo bridges $\text{V}-\text{O}-\text{P}$, whereas more acute values are observed for edge sharing (83.03°, 102.7°). The average P—O bond distances ($\bar{d}_{\text{P-O}} = 1.534$ Å) and intratetrahedral angles ($\bar{\alpha}_{\text{O-P-O}} = 109.4^\circ$) are in agreement with the reported values for orthophosphate compounds. At last, the mercury atoms exhibit the linear coordination found for mercurate HgO_2^{2-} anions with $\text{Hg}-\text{O}$ bond distances of ca. 2.1 Å and average $\text{O}-\text{Hg}-\text{O}$ bond angles of 171.7°. Additional oxygen atoms at distances greater than 2.7 Å complete the coordination sphere of the mercury species, and it is worthwhile to note that the oxygen O8 of the vanadyl group $\text{V}=\text{O}$ is at distances $d_{\text{Hg-O}} \sim 3$ Å from Hg1, Hg3, and Hg4. The four HgO_2^{2-}

(12) Blöchl, P. E.; Jepsen, O.; Andersen, O. K. *Phys. Rev. B* **1994**, *49*, 16223.

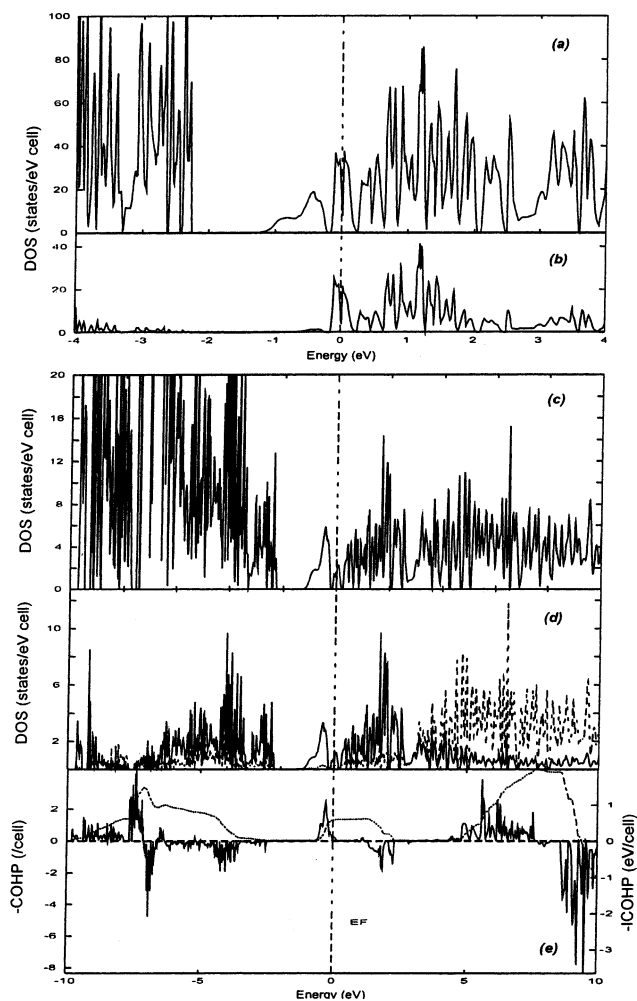
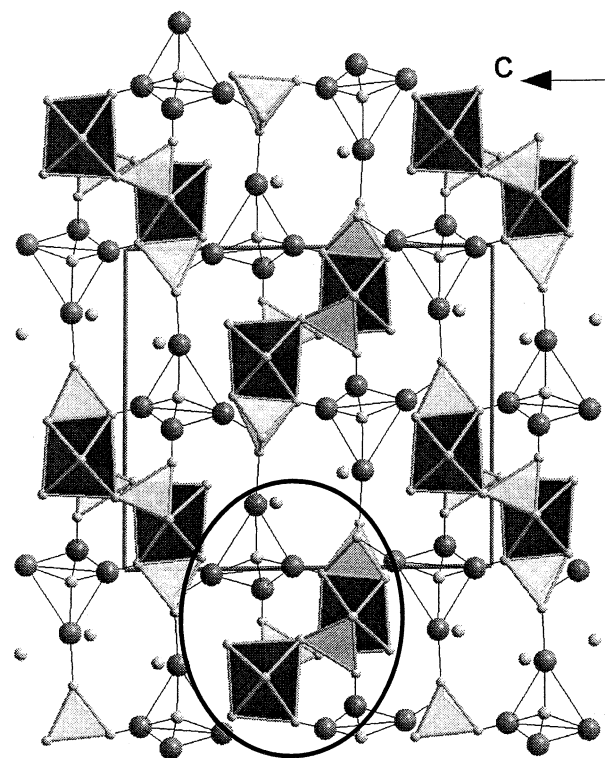


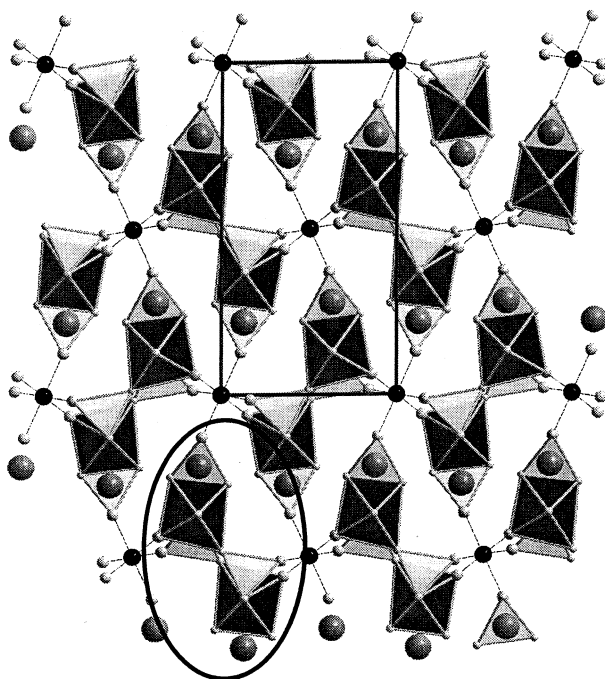
Figure 3. LMTO DOS and COHP for the model solid $\text{Hg}_4\text{O}(\text{VO})(\text{PO}_4)_2$: (a) total DOS, (b) V contribution, (c) Hg contribution, (d) Hg s (solid) and d (dotted) contributions, (e) Hg–Hg COHP (solid) and integrated COHP (dotted). The DOS and COHP curves have been shifted so that the Fermi level (indicated with a vertical dotted line) lies at 0 eV.

like units, directed grossly along the 3-fold axes of a tetrahedron, share one oxygen atom (O10) to form the unprecedented tetrahedral oxo-cluster Hg_4O_{-5} (Figure 2). The Hg–Hg bond distances from the edges of this oxo-cluster span the range 3.194–3.470 Å ($d_{\text{Hg-Hg}} = 3.36$ Å) and are longer than the distances found in metallic mercury ($d_{\text{Hg-Hg}} \sim 3$ Å), Hg_n^{x+} cations ($d_{\text{Hg-Hg}} \sim 2.5$ – 2.9 Å), or mercury-containing transition metal clusters ($\sim 2.7 \leq d_{\text{Hg-Hg}} \leq \sim 3.3$ Å).¹ This oxo-cluster is strongly bonded to PO_4 and VO_{5+1} to form a three-dimensional framework. The water molecule (Ow) is a near neighbor of Hg2 at a distance of 2.921(9) Å. Bond valence sum (BVS) calculations¹³ are in agreement with the formal oxidation states for the vanadium ($\sum s = 4.01$) and phosphorus centers ($\sum s = 5.02$ (P1), 5.00 (P2)). Similar calculations for the oxygen atoms have resulted in the electrostatic valence units (evu) 2.01 (O1), 1.83 (O2), 1.80 (O3), 1.84 (O4), 1.87 (O5), 1.81 (O6), 1.93 (O7), 1.74 (O8), 1.87 (O9), 1.98 (O10), and 0.10 (Ow). The calculated lack of ~ 1.90 evu for Ow clearly indicates the presence of a water molecule, as H^+ at about 1 Å from

(13) Brown, I. D.; Altermatt, D. *Acta Crystallogr.* **1985**, *B41*, 244.



(a)



(b)

Figure 4. Comparison of the structures of (a) $\text{Hg}_{4-x}\text{O}_{1-y}\text{VO}(\text{PO}_4)_2$ and (b) $\text{CaNiVO}(\text{PO}_4)_2$ (the NiO_6 octahedra are not represented for sake of clarity). The $[\text{VO}(\text{PO}_4)_2]_\infty$ chain is circled for both structures. Black polyhedra are octahedra VO_{5+1} ; open ones are tetrahedra PO_4 . Grey circles are the mercury or calcium atoms, black ones are nickel, and open ones are oxygen atoms and water molecules.

oxygen contributes ~ 0.9 valence units. In the case of mercury, the calculations were run according to N. E. Breese and M. O'Keeffe,¹⁴ and the formal oxidation states were,

respectively, 1.74 (Hg1), 1.53 (Hg2), 1.55 (Hg3), and 1.36 (Hg4), considering Hg^{2+} ($d(\text{Hg}-\text{O}) = 1.93 \text{ \AA}$) ($\langle \Sigma \text{Hg} = 1.69 \rangle$), and 1.61 (Hg1), 1.41 (Hg2), 1.43 (Hg3), and 1.26 (Hg4), considering Hg^+ ($d(\text{Hg}-\text{O}) = 1.90 \text{ \AA}$) ($\langle \Sigma \text{Hg} = 1.43 \rangle$). According to Brown and Altermatt,¹³ similar calculations lead to ($\langle \Sigma \text{Hg} = 1.69 \rangle$) considering Hg^{2+} ($d(\text{Hg}-\text{O}) = 1.972 \text{ \AA}$) values listed in Table 3. Obviously, the mercury ions do not adopt usual oxidation states, and from electroneutrality calculations, the $[\text{VO}(\text{PO}_4)_2]_{\infty}^{4-}$ chains are counterbalanced by tetrahedral cationic units $[\text{Hg}_{\sim 4}\text{O}_{\sim 1}]^{4+}$ that are consistent with mercury in the intermediate oxidation state $\sim 3/2$.

Periodic density functional calculations were carried out on the model compound $\text{Hg}_4\text{O}(\text{VO})(\text{PO}_4)_2$ to get a better knowledge of the bonding mode. Special attention was devoted to the $\text{Hg}_4(\mu_4\text{-O})\text{O}_4$ block that consists of the four linear HgO_2 groups (ML_2 type) sharing one oxygen atom. Some projected and total density of states (DOS) curves are shown in Figure 3. The Fermi level cuts a narrow peak centered on the d orbitals of the vanadium in agreement with the +4 formal oxidation state obtained from structure analysis (vide supra). Assuming that no interaction occurs between mercury atoms in the Hg_4O_5 block, the expected metallic electron count (MEC) is 40 as Hg^{2+} is normally required for stable HgO_2 groups.¹⁵ According to the structure results, the mercury is present as $\text{Hg}^{3/2+}$. Two additional electrons are therefore present on the Hg_4O_5 block with an MEC equal to 42. From the theoretical calculations, these two extra electrons occupy a narrow band just below the Fermi level. This band is centered on s and d_{z^2} orbitals of mercury as can be seen on the Hg projected DOS and the Hg–Hg crystal orbital Hamiltonian population (COHP) curves. Consequently, these extra electrons occupy bonding levels that strongly support the occurrence of Hg–Hg bonding within the Hg_4O_5 block. To the best of our knowledge, such an oxo-cluster is unique in solid-state chemistry, although organometallic compounds with similar tetrahedral Hg_4 units trapping carbon atoms (Hg_4C cores) were reported, but no Hg–Hg bondings were shown.¹⁶

The structure of $\text{Hg}_{4-x}\text{O}_{1-y}(\text{VO})(\text{PO}_4)_2 \cdot \text{H}_2\text{O}$ resembles to a large extent those of $\text{CaNi}[\text{V}^{\text{IV}}\text{O}(\text{PO}_4)_2]$ ¹⁷ and $\text{MV}^{\text{III}}[\text{V}^{\text{III}}\text{O}(\text{PO}_4)_2]$ with $\text{M} = \text{Ca}^{2+}$, Cd^{2+} , and Sr^{2+} ¹⁸ (Figure 4) that

were prepared by solid-state reactions. Indeed, all three structures show $[\text{VO}(\text{PO}_4)_2]_{\infty}^{x-}$ chains. These chains are connected through strong μ_2 -oxo bridges to $[\text{M}'\text{O}_4]_{\infty}$ rutile-like chains (Figure 4) of edge-sharing octahedra ($\text{M}' = \text{Ni}$, V) for $\text{CaNi}[\text{V}^{\text{IV}}\text{O}(\text{PO}_4)_2]$ and $\text{MV}^{\text{III}}[\text{V}^{\text{III}}\text{O}(\text{PO}_4)_2]$. The resulting three-dimensional open framework $\text{M}'[\text{VO}(\text{PO}_4)_2]^{2-}$ consists of tunnels that run along the [011] direction with Ca^{2+} , Cd^{2+} , and Sr^{2+} located within. The corresponding interactions are quite different in $\text{Hg}_{4-x}\text{O}_{1-y}(\text{VO})(\text{PO}_4)_2 \cdot \text{H}_2\text{O}$ as the cationic unit $[\text{Hg}_{\sim 4}\text{O}_{\sim 1}]^{4+}$ is connected to the chain $[\text{VO}(\text{PO}_4)_2]_{\infty}^{4-}$ through weak $\text{V}-\text{O}-\text{Hg}$ contacts ($d_{\text{Hg}-\text{O}} \sim 3 \text{ \AA}$) involving the oxygen atom from the vanadyl group and stronger $\text{P}-\text{O}-\text{Hg}$ links ($d_{\text{Hg}-\text{O}} \sim 2 \text{ \AA}$). At last, it is worthwhile to note that, though the chemical formula of the recently reported $\text{Hg}_4(\text{VO})(\text{PO}_4)_2$ ³ is very close to that of the title compound, their structures are very different. Indeed, homocondensation occurs in $\text{Hg}_4(\text{VO})(\text{PO}_4)_2$ that results in infinite chains of corner-sharing octahedra on one hand, the mercury atoms are present as Hg_2^{2+} dumbbells that connect the chains on the other hand, and the overall framework of $\text{Hg}_4(\text{VO})(\text{PO}_4)_2$ is two-dimensional.

Conclusion

The crystal structure of the new mercury vanadium phosphate hydrate has been solved. It consists of infinite chains $[\text{VO}(\text{PO}_4)_2]_{\infty}^{4-}$ that are built from fused distorted octahedra and tetrahedra. The chains are connected through strong $\text{P}-\text{O}-\text{Hg}$ links to the cationic unit $[\text{Hg}_{\sim 4}\text{O}_{\sim 1}]^{4+}$ and result in an overall three-dimensional open framework. Hg–Hg bondings within the oxo-cluster $[\text{Hg}_{\sim 4}\text{O}_{\sim 5}]$ have been proved from theoretical calculations. Comparison with the related vanadium phosphates $\text{CaNiVO}(\text{PO}_4)_2$ and $\text{MV}_2\text{O}(\text{PO}_4)_2$ is also presented.

Acknowledgment. The authors are indebted to Dr. T. Roisnel for the single-crystal intensity data collection on the Kappa CCD diffractometer (Université de Rennes, LCSIM, UMR 6511). E.F. and R.G. thank the Institut de Développement et de Ressources en Informatique Scientifique of Orsay (Project 000803) for computing facilities.

Supporting Information Available: Crystallographic data in CIF format. This material is available free of charge via the Internet at <http://pubs.acs.org>.

IC020229A

- (14) Breese, N. E.; O'Keefe, M. *Acta Crystallogr.* **1991**, *B47*, 192.
 (15) Allbright, T. A.; Burdett, J. K.; Whangbo, M. H. *Orbital interactions in Chemistry*; John Wiley and Sons: New York, 1985.
 (16) Grdenic, D.; Korpar-Colig, B.; Matkovic-Calogovic, D. *J. Organomet. Chem.* **1996**, *522*, 297 and references therein.
 (17) Meyer, S.; Müller-Buschbaum, Hk. *Z. Naturforsch.* **1997**, *52b*, 981.

- (18) Boudin, S.; Grandin, A.; Labbé, Ph.; Provost, J.; Raveau, B. *J. Solid State Chem.* **1996**, *127*, 325.